

# Modeling of groundwater salinity on the Persian Gulf coastal plain By using linear moments and ANFIS-PSO

Amir Jalalkamali<sup>1</sup>, Ali Sheykhbahaei<sup>2\*</sup>

<sup>1\*</sup> Department of water engineering, Kerman Branch, Islamic Azad University, Kerman, Iran, [ajalalkamali@yahoo.com](mailto:ajalalkamali@yahoo.com)

<sup>2</sup> Department of Nonliving Resources of Atmosphere and Ocean, Faculty of Marine Science and Technology, University of Hormozgan, Bandar Abbas, Iran Abbas, Iran, [Ali.sheikhbahaei@gmail.com](mailto:Ali.sheikhbahaei@gmail.com)

## ARTICLE INFO

### Article History:

Received: 21 Aug. 2021

Accepted: 31 Jul. 2021

### Keywords:

Salinity

ANFIS-PSO

Regional Analysis

At-Site Analysis

## ABSTRACT

The main source of water in Minab is the shallow aquifer which is part of the coastal aquifer. The quality of the groundwater is extremely deteriorated in terms of salinity. Salinization of groundwater may be caused and influenced by many variables. Studying the relation of between these variables and salinity is often a complex and nonlinear process, making it suitable for artificial intelligence application. The present paper presents a comparison of the hybrid of Adaptive Neuro Fuzzy Inference System (ANFIS) with Partial Swarm Optimization (PSO) model and L-moments regarding their power and efficiency in regional and at-site anticipation of salinity of groundwater at Minab coastal plain. In doing so, electrical conductivity is considered the dependent variable, while, through regression analysis, total cations, magnesium ion, sodium percentage, and level of groundwater are assumed to be independent parameters. Results showed that, in regions with lower heterogeneity criterion, ANFIS-PSO regional forecast were moderately more accurate than at-site anticipations.

## 1. Introduction

In many areas, especially in arid and semi-arid regions such as Minab coastal plain, groundwater is one of the main water resources for drinking water, agriculture, and industry uses. Aquifers and the contained groundwater are inherently sensitive to pollution from many sources. These days, Groundwater simulation has been used vastly for a better management of groundwater resources. Therefore, many researchers have tried to find more accurate models, considering the actual conditions. These models require plenty of information which is difficult and sometimes impossible to gather. Salinization may be caused by a number and/or combination of different processes, including: seawater intrusion; migration of brines from the deeper parts of the aquifer; dissolution of soluble salts in the aquifer (water-rock interaction); and contribution from discharges from older formations surrounding the coastal aquifer. In addition, potential man-induced (anthropogenic) sources include agricultural return flows, wastewater seepage, and disposal of industrial wastes. In addition, water quality (e.g. salinization) is influenced by many factors such as flow rate, contaminant load, medium of transport, water levels, initial conditions and other site-specific

parameters [1]. And also, considering some execution conditions, reaching a conclusion takes more time if possible at all. On the other hand, there are numerous factors in hydrologic parameters which complicate applying data to the models. Making physical and conceptual models have been poorly noticed for difficulty of gathering more information and the required time for calibration. In addition, nonlinearity of variables makes the problem more challenging. Recently, Artificial Intelligence (AI) models, as new powerful tools, have been used for forecasting hydrologic parameters. These methods act as a black box and do not require lots of physical data and are capable of estimating non-static water quality. Due to short processing time and low input data, AI models can supersede numerical ground water models. These new methods act as powerful estimators without the need for governing equations. For error reduction in regional forecasting, all selected wells must choose from one homogeneity cluster. So, it is necessary to define cluster homogeneity by some examinations. But one must make sure that these places are available. Because choosing some clusters with some wells inside is not sufficient for homogeneity. The L-moments as the new types of statistical methods act for solving such

problems. A quick search shows that regional forecasting with ANFIS-PSO is a new method for modeling. Nero-fuzzy networks for flood regional analysis were used [2]. Investigation shows that nero-fuzzy model versus artificial neural networks and non-linear correlation, has better ability in modeling of flood estimation in watersheds without hydrometer At-Sites. L-moments was investigated the great supply of four aquifers in Australia [3]. They found that regional analysis increase the accuracy of forecasting. Adaptive neuro fuzzy inference system (ANFIS) have been used to predict water supply in terms of quality and quantity trends in sophisticated systems with acceptable accuracy. [4, 5, 6, 7 and 8]. Methods of AI are nonlinear tools of modeling which do not need any explicit of the physical relationship of the problem. Through recent years, those successful applications for Soft Computing Techniques in the field of water engineering have been published in a great scale. [9, 10 and 11]. This paper attempts forecasting regional salinity of groundwater of Minab coastal plain by ANFIS-PSO with L-moments and comparison of between regional and At-Site results.

**2. Study area**

The Minab coastal plain is located in 56 ° 48' - 57 ° 15' E and 26 ° 1' - 27 ° 27' N. It covers a total area of 1378.8 square kilometers and its plain has an area of 788 square kilometers along the Persian Gulf. The maximum height of this plain is 50 meters and its minimum is zero. The main river is the Minab River (Fig. 1).



Figure1. Location of Minab coastal plain.

**3. Materials and methods**

**3.1. L-moments**

(Hosking, 1990) has a new definition of L-moments. Based on his studies, L-moments are analogous to traditional moments which are expressible as linear combinations of order statistics. Basically L-moments have linear functions as probability-weighted moments (PWMs) [12]. Alike conventional moments, the primary objective of PWMs and L-moments is to summarize previously-observed samples and theoretical distribution. The theory of PWM was summarized and defined by (Greenwood et al., 1979) as the following [13]:

$$\beta_r = E\{X[F_X(x)]^r\} \tag{1}$$

Where  $\beta_r$  is the  $r$ th order PWM and  $F_X(x)$  is the cumulative distribution function of  $X$ . Unbiased sample estimators (bi) of the first four PWMs are given as [14].

$$\begin{aligned} \beta_0 &= m = \frac{1}{n} \sum_{j=1}^n X_j \\ \beta_1 &= \sum_{j=1}^{n-1} \left[ \frac{n-j}{n(n-1)} \right] X_{(j)} \\ \beta_2 &= \sum_{j=1}^{n-2} \left[ \frac{(n-j)(n-j-2)}{n(n-1)(n-2)} \right] X_{(j)} \\ \beta_3 &= \sum_{j=1}^{n-3} \left[ \frac{(n-j)(n-j-1)(n-j-2)}{n(n-1)(n-2)(n-3)} \right] X_{(j)} \end{aligned} \tag{2}$$

Where  $x(j)$  represents the ranked AMS with  $x(1)$  being the highest value and  $x(n)$  the lowest value, respectively. The first four L-moment are given as follow

$$\begin{aligned} \lambda_1 &= \beta_0 \\ \lambda_2 &= 2\beta_1 - \beta_0 \\ \lambda_3 &= 6\beta_2 - 6\beta_1 + \beta_0 \\ \lambda_4 &= 20\beta_3 - 30\beta_2 + 12\beta_1 - \beta_0 \end{aligned} \tag{3}$$

Non-biased sample estimators in the first four L-moments are resulted by the substitution of the PWM sample estimators from Eq. (2) and Eq. (3). The first L-moment  $\lambda_0$  and the mean value of  $X$  are equal. At the end, the L-moment ratios are calculated as:

$$\begin{aligned} L-C_V &= \tau_2 = \frac{\lambda_2}{\lambda_1} \\ L-\gamma &= \tau_3 = \frac{\lambda_3}{\lambda_2} \\ L-k &= \tau_4 = \frac{\lambda_4}{\lambda_2} \end{aligned} \tag{4}$$

Sample estimates of L-moment ratios are obtained by substituting the L-moments in Eq. (4) with sample L-moments.

**3.2. Heterogeneity Measure**

Heterogeneity measure is used for identification of homogeneous regions based on observed and simulated dispersion of L-moments for a group of sites under consideration. This can be computed from [15]:

$$H = \frac{(V_1 - \mu_{V1})}{\delta_{V1}} \tag{5}$$

Where  $V$  = weighted standard deviation of values,  $\mu$  = the mean and standard deviation of  $N_{sim}$  values of  $V$ , and  $N_{sim}$  = number of simulations. A region is declared ‘acceptably homogeneous’ if  $H < 1$ ; ‘possibly heterogeneous’ if  $1 < H < 2$ ; and ‘definitely heterogeneous’ if  $H \geq 2$ . To avoid committing to a

particular 2 or 3 parameter distribution, simulation is undertaken using a 4 parameter Kappa distribution and the number of simulation is kept at least at 500 to arrive at reliable estimates of  $\mu$  and  $\sigma$ . In addition to the above, two additional measures H1 and H2 based on LCV/LCS and LCS/LCK distances respectively are also considered. The measure H1 indicates whether at-site and regional estimates will be close to each other, while H2 indicates whether the at-site and regional estimates will be in agreement. A large value of H1 usually indicates a large deviation between regional and at-site estimates, whereas a large value of H2 indicates a large deviation between at-site estimates and observed data.

### 3.3. Discordance Measure

Discordance measure, ZDIST, is used to screen out the data from unusual sites, i.e. sites whose at-site sample l-moments are markedly different from other sites and is defined as [16]:

$$D_i = \frac{1}{3}(u_i - \bar{u})^T \cdot S^{-1} \cdot (u_i - \bar{u}) \quad (6)$$

Where  $U_i$  = vector of LCV, LCS and LCK for a site  $i$ ;  
 $S$  = covariance matrix of  $V$ ;  $\bar{u}$  = mean of vector  $U_i$ .  
 A given site is declared discordant if  $D_i \leq 3$ . Critical value of ZDIST defines as [14]:

$$D_i \leq (n-1)/3 \quad (7)$$

Where  $n$  is number of At-Sites in studied region.

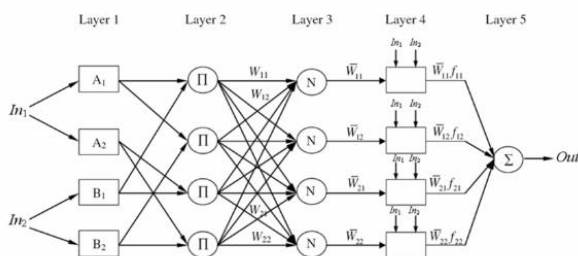


Figure 2. A typical ANFIS architecture for a two-input Sugeno model with four

### 3.4. The neuro-fuzzy structure

The ANFIS, the multilayer feed-forward network, maps inputs into an output using neural network learning algorithms and fuzzy reasoning. It is certain that a fuzzy inference system (FIS) is implemented in the framework of adaptive neural networks. Fig.1 illustrates the architecture of a typical ANFIS with five layers:

For simplicity, a typical ANFIS architecture with only two inputs leading to four rules and one output for the first order Sugeno fuzzy model is expressed [17,18]. It is also assumed that each input has two associated membership functions (MFs). It is clear that this architecture can be easily generalized to our preferred

dimensions. The detailed algorithm and mathematical background of the hybrid learning algorithm can be found in the Reference [18].

### 3.5. ANFIS-PSO method

There is a hybrid of canonical real-coded PSO, subtractive clustering and ANFIS, designed and finalized for the purpose of producing suitable approximate fuzzy models for the sake of accuracy and parsimony. The primary procedure of modeling is an optimization task executed by PSO where both the accuracy and compactness of fuzzy models are the subjects of simultaneous optimization. The whole process of optimization by PSO is based all particles that fly over the  $D$ -dimensional solution space are subject to updated rules for new positions, until the global optimal position is found. Velocity and position of a particle are updated by the following stochastic and deterministic update rules [19]:

$$v_i(t) = \omega v_i(t-1) + \rho_1 (x_{Pbest_i} - x_i(t)) + \rho_2 (x_{Gbest} - x_i(t)) \quad (8)$$

$$x_{i(t)} = x_i(t-1) + v_i(t) \quad (9)$$

where  $\omega$  is an inertia weight and  $r_1, r_2$  are random variables. The random variables are defined as  $U(0, 1)$ , and  $C1$  and  $C2$  are positive acceleration constants. Acceleration constants  $C1$  and  $C2$  represent the weights of the stochastic acceleration terms that push a particle toward  $Pbest$  and  $Gbest$ , respectively. The flow chart of modeling procedure is illustrated in Fig.3.

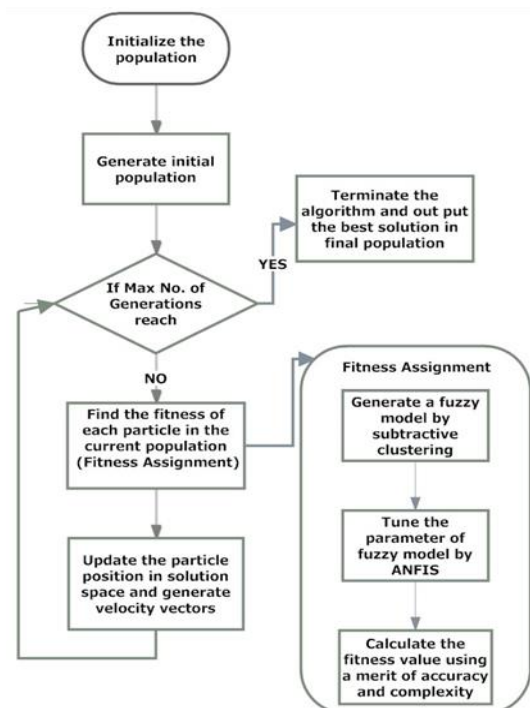


Figure 3. Steps of ANFIS-PSO model procedure

Subtractive clustering method can be used to generate a fuzzy model of TSK in which the number certain rules (i.e. the number of clusters) is determined through radii parameters dedicated into dimensions. These radii are mainly used for the purpose of cluster generation. Each cluster is meant to represent a rule and according to the fact that clustering is completed in multidimensional space, and fuzzy sets for each rule must be achieved. By projecting the center of each cluster in the corresponding dimension, the centers of MFs are obtained. The widths of MFs for a single dimension are obtained on the basis of radius  $r_a$  which is particularly considered for that dimension. Therefore, each chromosome in this study acts as radii values encoder for all dimensions inputs and outputs of a fuzzy model. These radii of fuzzy model are then used by subtractive clustering to generate a TSK FIS.

### 3.6. Simulation setup

The PSO algorithm parameters chosen for the tuning purpose are:  $ps = 100$ ,  $c_1$  and  $c_2 = 2$ ,  $w_{max} = 0.9$ ,  $w_{min} = 0.3$ . Number of epochs and learning rate are set to 100 and 0.2 for ANFIS. Ranges of radii are considered to be in interval [0.1, 2]. In the following subsections case studies are described in more detail.

### 4. Results and discussions

First step to define a homogenous region is choosing the most important clustering parameters. Choosing all important parameters to define a homogeneity cluster for a phenomena, increase calculating time and errors, so, choosing the most important parameters would make the calculation simpler, without resulting in any major differences. In this paper, out of effective parameters (time series parameters recorded) more important parameters were selected through regression analysis. Results showed that all of the cations, magnesium ions, sodium percentage, and groundwater level have more effect on salinity. Therefore, these parameters are used for electrical conductivity in clustering and also input parameters for forecasting. In this paper, with K-Means method and Ward hierarchical, the region was divided into 2, 3, and 4 sectors, respectively. And then, the incompatibility and non-homogeneity criteria for the region were defined. For choosing the best clustering mode and optimum number of regions, incompatibility summation of At-Sites, defining the number of incompatible At-Sites with more degree of 1.5, 2 and 3, and also non-homogeneity criteria were conducted for each and every region. Results are shown in Table.1

Considering Table.1, when all the At-Sites are considered as one region, only the H1 criteria are homogeneity while H2 and H3 are non-homogeneity. In general, K-mean method includes 4 regions as the priority and Ward, with 4 regions in the next place. Considering 4 homogeneity regions for research area, some wells were scattered in the other areas.

**Table 1. Non- homogeny criteria for different scenarios**

Criteria H <sub>3</sub>	Criteria H <sub>2</sub>	Criteria H <sub>1</sub>	Region	Method
6.77	2.5	1.5	Total	Total wells of a region
1.22	1.01	0.6	A	K-Means 2 region
2.5	-0.91	-0.45	B	
1.3	0.65	0.4	A	K-Means 3 region
2.28	-0.53	-0.25	B	
3.29	-0.99	-0.45	C	
0.88	0.15	0.1	A	K-Means 4 region
1.01	-0.35	-0.25	B	
0.9	-0.22	-0.11	C	
1.8	0.45	0.12	D	
1.22	1.01	0.6	A	Ward 2 region
2.5	-0.91	-0.45	B	
1.21	0.59	0.32	A	Ward 3 region
2.33	-0.43	-0.31	B	
1.09	-0.71	-0.33	C	
0.92	0.23	0.14	A	Ward 4 region
1.17	-0.25	-0.41	B	
1.29	-0.31	-0.14	C	
1.96	0.69	0.45	D	

To solve this problem, all the following, well No3 in region A, well No15 in region B, and well No27 in region D were combined together and then the non-homogeneity criteria were computed. Relocation of the wells increased the non-homogeneity of region A and B and decreased that of region C. To define the increase of non-homogeneity, incompatibility of the wells was investigated and it was observed that well No14 was incompatible. The well was moved to region B and computation was restarted. The results showed decreased incompatibility for well No14. And finally, with moving to region B and re-computation, better results were achieved. Figures below show the final homogeneity regions.

#### 4.1. Regional forecasting

First and foremost, for regional forecasting, dimensionless data was computed in each one of the three regions including both selection input data and electrical conductivity. After choosing the best scenario for forecasting, by multiplying average off each well by regional dimensionless data, the dimensionless forecasting data is obtained for each well. Desired periodical statistics are considered on a monthly basis from 2001 to 2013. For analysis, 156 regional dimensionless data were used. In this research, 70 percent of the data was used for teaching, 10 percent for validation, and the remaining 20 percent was used

for the testing. Furthermore, for regional forecasting, models constructed with the relation equation are studied. In all models, the momentum training and ANFIS-PSO method were used.

**Table 2. The best topology of ANFIS-PSO model for the study areas**

Region	Model	NO. OF INPUT VARIABLE	NO. OF RULES	No. of MF	R <sup>2</sup>
A	ANFIS-PSO	4	6	24	0.9765
B	ANFIS-PSO	4	5	20	0.9956
C	ANFIS-PSO	4	3	12	0.9949

Having observed the results of correlation coefficient and non-homogeny criteria, it is obvious that non-homogeny decreased, the correlation coefficient of the observed data and regional forecasted data decreased as well. The reason is that low non-homogeny means incompatibility of the wells with the other wells in the same region. So, this would be able to reduce forecasting error. After implementing the proposed method (ANFIS-PSO) for each region, with multiplying the coefficient of each At-Site for the desired year, by regional forecasting data, electrical conductivity was calculated for each At-Site, and, finally, between the observed and calculated data, the correlation coefficient was calculated. Tables 4 to 6 show the correlation coefficient for each well.

**Table 3. The correlation coefficient between observed and predicted data for each well in the area A**

R <sup>2</sup>	Well number	R <sup>2</sup>	Well number
0.97	8	0.86	1
0.90	9	0.91	2
0.92	10	0.77	3
0.94	11	0.93	4
0.99	12	0.95	5
0.89	13	0.97	6
		0.90	7

**Table 4. The correlation coefficient between observed and predicted data for each well in the area B**

R <sup>2</sup>	Well number	R <sup>2</sup>	Well number
0.90	19	0.98	14
0.92	20	0.79	15
0.91	21	0.99	16
0.96	22	0.99	17
		0.86	18

**Table 5. The correlation coefficient between observed and predicted data for each well in the area C**

R <sup>2</sup>	Well number	R <sup>2</sup>	Well number
0.91	29	0.85	23
0.98	30	0.86	24
0.95	31	0.93	25
0.98	32	0.93	26

0.84	33	0.73	27
0.99	34	0.90	28

Considering the results shown in tables 3, 4, and 5 the wells No3, No15 and No27 which were moved before, have the least correlation coefficient. Better correlation coefficients are associated with the wells with salinity levels close to that of the regional average. Thus, it follows that regional analysis can forecast with high precision, in case of selection of wells and internal At-Sites. Figures 4 and 5 show forecasting and regional salinity. According to figures, it would be useful to reduce the abstraction rate and increase the recharge quantities (the groundwater level) to the aquifer as a strong remedial action for solving the groundwater deterioration problem in the aquifer of Minab coastal plain (salinity).

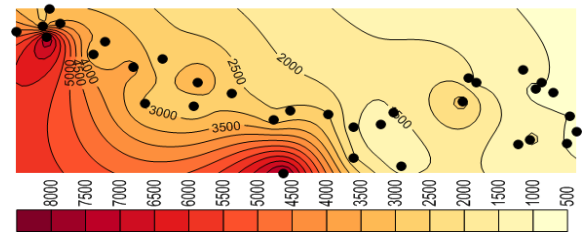


**Figure 4. Observed salinity for September 2013**

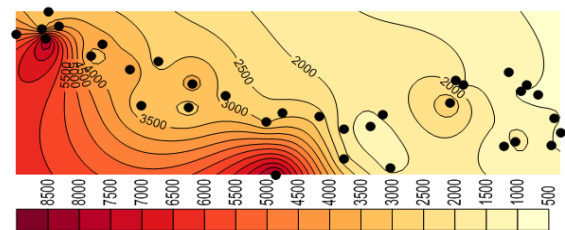


**Figure 5. Predicted salinity for September 2013**

#### 4.2. At-Site forecasting

For forecasting the salinity of our 34 wells, similar to the regional method, the proposed method ANFIS-PSO is applied to each well. For this purpose, the correlation coefficient between the observed data and forecasted data was obtained. After choosing the appropriate model, the forecasting started. Review of the results suggests that the salinity of groundwater for the study area increased during the past years. And also it's clear that ANFIS-PSO is capable of forecasting acceptable groundwater salinity.

#### 4.3. Comparison of At-Site and regional forecasting

Priority of regional or At-Site analysis for each studied well of Minab plain was revealed through the method of correlation of coefficient, and then inserted into Table 6.

**Table 6. Correlation coefficient for best structures at different**

Priority	Correlation Coefficient		Well No
	Regional	At-Site	
At-Site	0.86	0.95	1
At-Site	0.91	0.98	2
At-Site	0.78	0.83	3
At-Site	0.93	0.95	4
At-Site	0.95	0.96	5
Regional	0.98	0.91	6
Regional	0.90	0.82	7
Regional	0.97	0.89	8
At-Site	0.91	0.95	9
Regional	0.92	0.91	10
Regional	0.94	0.89	11
Regional	0.98	0.92	12
Regional	0.89	0.81	13
Regional	0.98	0.83	14
At-Site	0.79	0.87	15
Regional	0.98	0.9	16
Regional	0.99	0.94	17
Regional	0.86	0.85	18
At-Site	0.90	0.96	19
Regional	0.82	0.88	20
Regional	0.91	0.93	21
At-Site	0.93	0.93	22
At-Site	0.85	0.81	23
Regional	0.87	0.93	24
Regional	0.93	0.94	25
Regional	0.93	0.89	26
At-Site	0.73	0.8	27
At-Site	0.90	0.87	28
Regional	0.91	0.91	29
Regional	0.95	0.95	30
Regional	0.94	0.94	31
Regional	0.98	0.95	32
At-Site	0.83	0.95	33
Regional	0.98	0.97	34

According to the results mentioned above, 21 wells with regional analysis and 13 wells with At-Site analysis method maintain good accuracy. The investigation shows that for wells, for which regional analysis shows lower accuracy in comparison to At-Site analysis, the average is above regional average (wells No<sub>1</sub>, No<sub>5</sub>, No<sub>9</sub>, No<sub>15</sub>, No<sub>19</sub> and No<sub>22</sub>) or below regional average (wells No<sub>23</sub>, No<sub>28</sub> and No<sub>33</sub>). The rate of incompatibility for these wells is higher than the other regional homogenous wells. Region A has the most priority in At-Site analysis followed by C and D. As a result, the most important regions for analysis are the non-homogenous regions. As a result, in case of

proper selection of the at-sites in a homogeneous region and low at-sites incompatibility as well as non-homogeneity criterion, regional analysis is preferable to at-site analysis.

### 5. Conclusion

The current research showed that hybrid models can be used in groundwater quality management and outcome is comparable to other used approaches such as groundwater numerical modelling. According to regression analysis, sum of cations, magnesium ions, percentage of sodium, and groundwater table are the most effective on salinity. Moreover, for defining the number of homogeneity clusters, generally, K-Means method, with 4 regions is the first and Ward with 4 regions is the second suitable selection. As the non-homogeneity criteria decreased, correlation coefficient between the observed data and regional forecasted data reduced as well. The largest correlation coefficient was associated to the wells with close salinity to the regional average. In case of precise selection of the wells and At-Sites inside the region, the regional analysis can forecast with high accuracy. The most important regions for analysis are the non-homogenous regions. Forasmuch as, the PSO, which is a global random optimization algorithm, can simultaneously identify system structure and parameters. Therefore, the ANFIS-PSO model analysis showed an increase in the compactness and accuracy of the mentioned model during the testing stage. Our proposed method aiming to provide us with the best and effective composition of structure in the ANFIS model exchange rise and fall between the precision and the simplicity. The maintained results are to show a new hybrid algorithm providing both accuracy and complexity for a Neuro-Fuzzy model.

### References

- [1] Govindaraju R. S., (2000). "Artificial neural network in hydrology". Journal of Hydrologic Engineering, 5(2), 124-137.
- [2] Shu, C., Ouarda, T.B.M.J. (2008). Regional flood frequency analysis at engaged sites using the adaptive neuro-fuzzy inference system. Journal of Hydrology., V.349, PP.31-43.
- [3] Furst, j., Bichler, A. and Konecny, F. (2014). Regional Frequency Analysis of Extreme Groundwater Level. Journal of Grounwater, Jonwielly.
- [4] Jalalkamali, Amir., Sedghi, Hossein., Manshour, Mohammad .(2011)., Monthly groundwater level prediction using ANN and neuro-fuzzy models: a case study on Kerman plain, Iran, Journal of hydroinformatics (13.4) 867-876.
- [5] Adamowski, Jan., Fung Chan, Hiu. (2011)., A wavelet neural network conjunction model for groundwater level forecasting, Journal of Hydrology (407) 28-40.
- [6] Lohani, AK., Krishan, G. (2015) Application of artificial neural network for groundwater level simulation in Amritsar and Gurdaspur districts of Punjab, India. Journal of Earth Science and Climate Change 6:274.

- [7] Samson, M., Swaminathan, G., Venkat Kumar, N. (2010)., Assessing groundwater quality for portability using a Fuzzy logic and GIS – a case study of Tiruchirappalli city – India, *Computer Modeling and New Technologies*, Vol.14, No.2, 58–68.
- [8] Jalalkamali, Amir. (2015)., Using of hybrid fuzzy models to predict spatiotemporal groundwater quality parameters, *Earth Science Informatics*, DOI 10.1007/s12145-015-0222-6.
- [9] Jalalkamali, Amir. Moradi, Mehdi., Moradi, Nasrin. (2015)., Application of several artificial intelligence models and ARIMAX model for forecasting drought using the Standardized Precipitation Index, *International Journal of Environmental Science and Technology*, Volume 12, Issue 4, pp 1201-1210.
- [10] Lohani, A.K., Krishan, G. (2015)., Groundwater Level Simulation Using Artificial Neural Network in Southeast, Punjab, India, *Journal of Geology & Geophysics* 4: 206.
- [11] Seyam, Mohammed., Mogheir, Yunes. (2011). A NEW APPROACH FOR GROUNDWATER QUALITY MANAGEMENT, *the Islamic University Journal (Series of Natural Studies and Engineering)*, Vol.19, No.1, pp 157-177.
- [12] Hosking, J.R.M. (1990). L-moments: Analysis and estimation of distributions using linear combinations of order statistics: *J.R. Stat. Soc., Ser. B*, 52, 105-124.
- [13] Greenwood, J.A., Landwehr, J.M., Matalas, N.C., and Wallis, J.R. (1979). Probability weighted moments: Definition and relation to parameters of several distributions expressible in inverse form. *Water Resources Research*, 15(5), 1049-1054.
- [14] Hosking, J. R. M., & Wallis, J. R. (1997). *Regional Frequency Analysis: An Approach Based on L-Moments*. Cambridge Univ. Press, New York.
- [15] Kjeldsen, T. R., Jones, D. A. (2006). Prediction uncertainty in a median-based index flood method using L- moments. *Water Resources Research*, V. 42.
- [16] Rostami, R., & Rahnama, M. B. (2007). Halil-river Basin regional flood frequency analysis based on l-moment approach. *International journal of agriculture researches*, USA, Newyork.
- [17] Sugeno, M. (1985) *Industrial applications of fuzzy control*. Elsevier Science Pub.Co.
- [18] Wang, Y.M., Elhag, T. (2008) An adaptive neuro-fuzzy inference system for bridge risk assessment. *Expert Systems with Applications* 34(4): 3099-3106.
- [19] Jang JSR. (1993) ANFIS: Adaptive-network-based fuzzy inference systems, *IEEE Transactions on Systems Man and Cybernetics*, 23 (3), pp 665–685.
- [20] Kennedy J, Eberhart R (1995) Particle swarm optimization. In: *Proceedings of the IEEE international conference on neural networks*, Perth, pp 1942–1948 Z.